

## CONTENTS – A through B

---



---

A New Method for the Extraction of the Metal Particles of Ordinary Chondrites: Application to the Al Kidirite (H6) and New Halfa (L4) Meteorites <i>Y. A. Abdu</i> .....	5033
Geophysical Signature of Serra Da Cangalha Impact Crater, Brazil <i>A. A. Abraham, J. M. Flexor, and S. L. Fontes</i> .....	5167
Characterization of Matrix in the EET92042 CR2 Carbonaceous Chondrite: Insights into Textural and Mineralogical Heterogeneity <i>N. M. Abreu and A. J. Brearley</i> .....	5178
Mass Fractionation of Fe and Ni Isotopes in Metal in Hammadah Al Hamrah 237 <i>C. M. O'D. Alexander and R. H. Hewins</i> .....	5080
Monocarboxilic Acids Analyse in Murchison Meteorite Using Solid Phase Microextraction (SPME) <i>M. R. Alexandre, Y. Huang, Y. Wang, M. Fuller, and S. Pizzarello</i> .....	5082
Isotopic Study of Presolar Graphite in the KFC1 Separate from the Murchison Meteorite <i>S. Amari, E. Zinner, and R. S. Lewis</i> .....	5152
The Poty Quarry Conglomeratic Bed: The Record of a Tsunami Triggered by an Impact? <i>J. A. Barbosa and V. H. Neumann</i> .....	5230
What does the CM Chondrite Mineralogic Alteration Index Really Mean? <i>G. K. Benedix and P. A. Bland</i> .....	5184
Exploring the Possible Connection Between Ordinary Chondrites and Primitive Achondrites <i>G. K. Benedix, R. Ford, T. J. McCoy, T. Rushmer, and C. M. Corrigan</i> .....	5179
Abundance and Meaning of Regolith Breccias Among Meteorites <i>A. Bischoff and L. Schultz</i> .....	5118
The Production Rate of Small Craters on Earth, and the Expected Crater Population in South America <i>P. A. Bland, N. A. Artemieva, and C. R. de Souza Filho</i> .....	5164
Maps of Elemental Abundances on the Surface of Mars <i>W. Boynton, D. Janes, K. Kerry, K. Kim, R. Reedy, L. Evans, R. Starr, D. Drake, J. Taylor, and H. Wänke</i> .....	5206
Cathodoluminescence Study of Albite Feldspars and Ca-Phosphates in Type 4–6 Ordinary Chondrites <i>F. Brandstätter</i> .....	5122
Petrographic Classification and Chondrule Textures of Fossil Meteorites from Southern Sweden <i>J. C. Bridges, B. Schmitz, and R. Hutchison</i> .....	5154
Olivine Decomposition Features in the Y000593 and NWA998 Nakhrites <i>J. C. Bridges, P. H. Warren, and M. R. Lee</i> .....	5140

An Ion Probe Study of the Sulphur Isotopic Composition of Fe-Ni Sulphides in CM Carbonaceous Chondrites <i>E. S. Bullock, K. D. McKeegan, M. Gounelle, M. M. Grady, and S. S. Russell.....</i>	5172
Two Large Moroccan Mesosiderites: NWA 1817/1878/1979/2042 and NWA 1827/1879/1882/1912/1951/1982/3055 <i>T. E. Bunch, A. J. Irving, J. H. Wittke, and S. M. Kuehner.....</i>	5163
Near-Infrared Spectroscopy of Vestaoids <i>T. H. Burbine, T. J. McCoy, J. M. Sunshine, A. S. Rivkin, R. P. Binzel, and S. J. Bus .....</i>	5209
Noble Gases from the Interstellar Medium Trapped on the MIR Space Station and Analyzed by In Vacuo Etching <i>H. Busemann, F. Bühler, Y. N. Agafonov, H. Baur, P. Bochsler, N. A. Eismont, V. S. Heber, R. Wieler, and G. N. Zastenker .....</i>	5170
Constant Sunlight at the Lunar North Pole <i>D. B. J. Bussey, K. Fristad, P. Schenk, M. S. Robinson, and P. D. Spudis.....</i>	5181
Mössbauer Studies in Impactites from Huamalies Province in Huancavelica Region, Peru <i>A. Bustamante, S. Espinoza, G. Morales, and R. B. Scorzelli .....</i>	5102

## A NEW METHOD FOR THE EXTRACTION OF THE METAL PARTICLES OF ORDINARY CHONDRITES: APPLICATION TO THE AL KIDIRATE (H6) AND NEW HALFA (L4) METEORITES.

Y. A. Abdu. Department of Earth Sciences, Uppsala University, 752 36 Uppsala, Sweden. E-mail: yassir.abdu@geo.uu.se.

The metal in iron, stony-iron, and the metal particles in chondrites is basically composed of two Fe-Ni minerals: *kamacite*, the (BCC) phase, with ~ 5-7 at% Ni and *taenite*, the (FCC) phase, normally with ~ 25-50 at% Ni. Taenite from slowly cooled meteorites contains in its microstructure some special Fe-Ni phases, which are formed at low temperatures (below ~ 400 °C). For example, the atomically ordered  $\text{Fe}_{50}\text{Ni}_{50}$  phase (*tetrataenite*) and the paramagnetic phase or low-Ni taenite with ~ 25 at% Ni (*antitaenite*). Rancourt and Scorzelli [1] proposed the intergrowth of tetrataenite and antitaenite as a possible equilibrium state at ~ 20-40 at% Ni.

Mössbauer spectroscopy has been used extensively for studying taenite from iron and stony-iron meteorites [2]. However, the study of taenite from the metal particles of ordinary chondrites has, in part, been hampered by the presence of the silicates and troilite phases, which dominate the Mössbauer spectrum of the whole rock powdered samples. Furthermore, ordinary chondrites contain small amounts of taenite, which is more abundant in the LL chondrites and decreases in abundance through the L to H chondrites.

Recently, we have developed a simple magnetic separation method for the extraction of the metal particles of ordinary chondrites, then dissolved kamacite in conc. HCl to obtain taenite-enriched samples [3]. The whole rock powdered sample is first subjected to magnetic separation in acetone using a hand magnet. The magnetic fraction is then taken and submitted to further grinding and magnetic separation in acetone several times in order to purify the metal particles from silicates and troilite. The Mössbauer spectra of the metal particles extracted from the Al Kidirate (H6) and New Halfa (L4) chondrites, using the above method, contain kamacite (the dominant phase) and small amounts of taenite and antitaenite. In order to explore the presence of tetrataenite in these samples, the purified metal particles are chemically treated in conc. HCl at ~ 50 °C for a few hours. The Mössbauer spectra of the resulting taenite-enriched samples identify the following Fe-Ni phases: tetrataenite, disordered  $\text{Fe}_{50}\text{Ni}_{50}$  taenite, antitaenite, and small amounts of kamacite/martensite. The Al Kidirate sample contains ~ 50 % of tetrataenite, which is surprisingly high for an H chondrite. The presence of abundant disordered taenite (~ 30 %) coexisting with tetrataenite (~ 29 %) in the metal particles of the New Halfa indicates that the parent body of New Halfa may have experienced shock and re-heating events, consistent with the shock stage S3 (~ 15-20 GPa) reported for this meteorite [4].

The application of high field Mössbauer spectroscopy to these samples at room temperature resulted in large induced magnetic moments in antitaenite. The results, when compared to synthetic Fe-rich Fe-Ni alloys [5], may be used to estimate the Ni content of antitaenite in meteorites, which depends on the cooling history of meteorites below 400 °C. **References:** [1] Rancourt D. G. and Scorzelli R. B. 1995. *Journal of Magnetism and Magnetic Materials* 150:30. [2] Knudsen J. M. 1989. *Hyperfine Interactions* 47:3. [3] Abdu Y. A. et al. 2002. *Hyperfine Interactions (C)* 5:375. [4] Wlotzka F. 1995. *Meteoritics* 30:794. [5] Abdu Y. A. et al. 2004. *Journal of Magnetism and Magnetic Materials*. In press.

**GEOPHYSICAL SIGNATURE OF SERRA DA CANGALHA IMPACT CRATER, BRAZIL.**

A.A. Abraham, J.M. Flexor and S. L. Fontes. Observatório Nacional/MCT, Brazil. E-mail: [flexor@on.br](mailto:flexor@on.br)

A geophysical signature of Serra da Cangalha impact crater located in the southwestern region of the Parnaíba Basin, Brazil, is presented. This signature was established by an integration of magnetotelluric (MT) sounding data (2-D inversions and 3-D forward modeling) and aeromagnetic data (location and depth of magnetic sources in the crater by Euler deconvolution method). The MT survey was carried along three radial profiles trending NW-SE, ENE-WSW and NNE-SSW across the crater. For MT sites located further away from the centre of the crater, isotropic MT responses were observed, suggesting a 1D conductivity distribution in the subsurface in the frequency range of 100 to 10 Hz. For sites located in the vicinity of the inner ring of the crater, anisotropic responses were observed in the same frequency range. A 2D resistivity inversion of MT data [1] reveals a four-layer model for the three profiles, representing a thin resistive layer underlain by a conductive layer, a weathered basement and a resistive crystalline basement. The depth to top of the basement is estimated to be about 1.2 km in good agreement with information available for nearby wells. The structure is interpreted to have a diameter of about 13 km with a central uplift of the basement. However, in view of the circular geometry of the crater, we carried out a 3D forward modeling computation to supplement the derived 2D model. The 3D resistivity forward model [1], fitting the MT responses by trial-and-error, shows a significant reduction in the basement resistivity around the center of the crater, probably caused by the impact-induced fracturing of the subsurface. The solutions obtained by Euler deconvolution of aeromagnetic data have shown magnetic sources which can be related to the impact structure whose depths varies between 0.8 to 2.5 km. The circular geometry of the crater is well delineated. Also, the downward continuation of the aeromagnetic data showed clearly at 1.1 km depth a magnetic anomaly related to an uplifted basement most probably due to meteorite impact.

**Reference:** [1] Rodi W and Mackie R.L. 2001. *Geophysics* 66 : 174-187.

## CHARACTERIZATION OF MATRIX IN THE EET92042 CR2 CARBONACEOUS CHONDRITE: INSIGHTS INTO TEXTURAL AND MINERALOGICAL HETEROGENEITY

Neyda M. Abreu and Adrian J. Brearley. Dept. of Earth and Planetary Sciences, University of New Mexico, Albuquerque, NM 87131, USA; [abreu@unm.edu](mailto:abreu@unm.edu).

**Introduction:** CR2 chondrites are a group of primitive carbonaceous chondrites that record a variety of early solar system processes. In particular, the CR2 chondrites show varying degrees of aqueous alteration, that has affected fine-grained matrices and, to a lesser extent, chondrules [1,2]. At present our understanding of the effects of progressive aqueous alteration on the mineralogy of CR matrices is incomplete. Here we report preliminary SEM and EPMA results of matrix in EET92042, a CR chondrite that has not been studied in detail.

**Results:** SEM studies show that, like other CR chondrites, EET 92042 is a breccia [1]. Mineral and lithic fragments are common in some regions of the matrix and dark inclusions (DIs) also occur. The matrix shows considerable textural and mineralogical heterogeneity from region to region. Most areas of matrix are similar to other CR matrices [2,3,4], indicated by fine-grained magnetite frambooids and platelets, calcite and sulfides (~1-5 m). These phases are embedded within a groundmass that is too fine-grained to resolve in detail by SEM, but may consist of phyllosilicates. These areas of matrix are texturally distinct from fine-grained rims that are present on some chondrules. Other regions of the matrix of EET92042 are dominated by relatively coarse-grained materials that show a distinct preferred alignment. Observations from one DI show that it is finer-grained than the host meteorite, with only minor magnetite, but relatively abundant calcite. The boundary between the DI and the host chondrite matrix is gradational in character. EMPA analyses show the DI has essentially the same major element composition as the matrix, consistent with the results of [4,5]. However, fine-grained rims are notably lower in Mg, S and Ni than either typical regions of matrix or the DI.

**Discussion:** These studies show that matrix in EET92042 is textural and mineralogical complex and has been affected by a number of different processes. First, it is clear that there are primary heterogeneities in the matrix composition. For example, fine-grained rims are texturally and compositionally distinct from adjacent matrix and these differences have been preserved during aqueous alteration. Second, the effects of brecciation/shock have caused significant modification of the matrix, at least on a localized scale, as indicated by the local fabrics, particular around chondrule boundaries. Brecciation has also formed regions of matrix that are highly clastic in character. Although there are distinct regions of matrix in EET92042, there are no clearly defined boundaries between one type of matrix and another. It is possible that some of the heterogeneity is the result of fine-scale regolith mixing of clasts of CR-related materials that have experienced different degrees of alteration, but if this is the case, then the boundaries between these clasts have been obscured by some later process, such as continued aqueous alteration and/or brecciation that resulted in final lithification of the meteorite.

**References:** [1] Weisberg, et al. (1993). *GCA* **57**, 1567-1586. [2] Ichikawa, O. and Ikeda, Y. (1995). *Proc. NIPR Symp. Antarct. Meteorites* **8**, 63-78. [3] Krot et al. (2002). *MAPS* **37**, 1451-1490. [4] Zolensky, et al. (1993). *GCA* **57**, 3123-3148. [5] McSween and Richardson (1977). *GCA* **41**, 1145-1161.

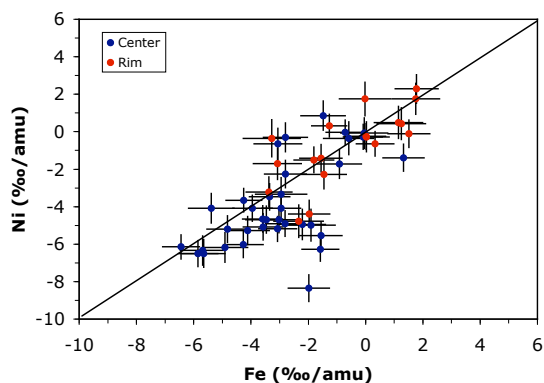
**Acknowledgements:** This research was supported by NASA grant NAG5-13444 (A. J. Brearley, P.I.).

## MASS FRACTIONATION OF Fe AND Ni ISOTOPES IN METAL IN HAMMADAH AL HAMRAH 237.

C. M. O'D. Alexander<sup>1</sup> and Roger H. Hewins<sup>2</sup>. <sup>1</sup>Dept. of Terrestrial Magnetism, Carnegie Institution of Washington, 5241 Broad Branch Rd. N.W., Washington DC 20015, USA. [alexande@dtm.ciw.edu](mailto:alexande@dtm.ciw.edu). <sup>2</sup>Dept. of Geological Sciences, Rutgers University, 610 Taylor Rd., Piscataway NJ 08855, USA

**Introduction:** A number of CH and some “CB” chondrites contain zoned Fe-Ni metal grains, with Ni- and refractory PGE-rich cores [1-4]. They have been explained by near-equilibrium to disequilibrium condensation from solar to lithophile-enriched gas. We analyzed Hammadah al Hamra 237 in search of additional constraints for the conditions of formation of its zoned metal.

**Results:** The Ni-rich cores are easily identified in BSE. This metal has up to 12% Ni and has experienced minor exsolution, whereas rims and unzoned metal have down to 6% Ni. Iron and Ni isotope analyses were performed using the Carnegie Cameca IMS 6f ion probe at a mass resolution of ~8000. The standards were Nelson County (IIIF) and NBS126C, a high Ni steel.



Iron and Ni show large, correlated mass fractionations, with a total range of ~8‰/amu. On average, the cores have lighter isotopic compositions than the rims. Under Rayleigh conditions, Fe and Ni condensation produces roughly a -8 to -9‰/amu fractionation in condensates relative to the gas. This meteorite also has a negative bulk  $\delta^{65}\text{Cu}$  [5]. The Fe, Ni and Cu isotopes all suggest that the metal in HH 237 formed by rapid, disequilibrium condensation.

**References:** [1] Weisberg M. K. and Prinz M. 1999. *Proc. NIPR Symp. Antarc. Meteor.* 30:189–190. [2] Meibom A. et al. 1999. *Journal of Geophysical Research* 104:22053–22059. [3] Campbell A. J. et al. 2001. *Geochim. Cosmochim. Acta* 65:163–180. [4] Petaev M. I. et al. 2003. *Geochimica et Cosmochimica Acta* 67:1737–1751. [5] Russell, S. S et al. 2003. *Meteoritics & Planetary Science* 38:A124.

**MONOCARBOXILIC ACIDS ANALYSE IN MURCHISON  
METEORITE USING SOLID PHASE  
MICROEXTRACTION (SPME)**

M. R. Alexandre<sup>1,3</sup>, Y. Huang<sup>1</sup>, Y. Wang<sup>1</sup>, M. Fuller<sup>1</sup>, and S. Pizzarello<sup>2</sup>. <sup>1</sup>Department of Geological Sciences, Brown University, Providence, RI 02906. <sup>2</sup>Department of Chemistry & Biochemistry, Arizona State University, Tempe, AZ 85287, <sup>3</sup>Departamento de Química, Universidade Federal de Santa Catarina, Brasil, 88040 900. E-mail: marcelo\_qmc@yahoo.com.br

**Introduction:** Low molecular weight monocarboxylic acids (MCAs) are the most abundant soluble organic compounds in the Murchison [1,2] and other CM carbonaceous chondrites [3,4]. However, there are concerns from the experimental procedures used to isolate MCAs for GC and GCMS analysis in the early studies on the Murchison. The procedure involved a water-CH<sub>2</sub>Cl<sub>2</sub> partitioning step to extract the MCAs, followed by solvent evaporation prior to GC and GCMS analyses. Because the low molecular weight acids are miscible with water and highly volatile, the procedure is likely to cause significant loss of MCAs and results in bias in molecular distributions. Later study using cryogenic distillation and ion chromatography [1,5] indeed demonstrated that a major loss in acetic acid in the earlier report must have occurred. In this study, we examined the monocarboxylic acids in Murchison meteorite using a new sample preparation and introduction technique for gas chromatograph recently developed for volatile, water-soluble organic compounds: solid phase micro-extraction (SPME).

**Results and Discussions:** Using SPME coupled with GC, GCMS, we found a much larger suite of more than 50 straight chain and branched monocarboxylic acids. The straight chain monoacids range from C<sub>1</sub> to C<sub>10</sub> and the branched monoacids were found in a complete structural diversity. Identifications were carried out by coinjection with authentic standards, by comparing mass spectra using computer library and published GC retention times [3,4] and interpretation of mass spectra. We used a 70 mm Carbowax<sup>TM</sup>/DVB StableFlex<sup>TM</sup> SPME fiber which was held by an SPME fiber assembly (Supelco). To obtain the optimum conditions for the extraction efficiency, and consequently better identification and quantification, we tested a series of experimental conditions for adsorption and desorption using an aqueous solution containing 6 C<sub>2</sub> to C<sub>6</sub> monocarboxylic acid standards (concentrations ~ 1mmol/L in water)[7,8]

**References:** [1] Yuen G. and Kvenvolden K. A. (1973) *Nature*, 246, 301-302. [2] Lawless J. G. and Yuen G. (1979) *Nature*, 282, 396-398. [3] Shimoyama et al. (1989) *Geochem. J.*, 23, 181-193. [4] Naraoka et al. (1999) *Origins of Life and Evolution of the Biosphere*, 29, 187-201. [5] Yuen G. et al. (1984) *Nature* 307, 252-254. [6] Lord H. and Pawliszyn (2000) *J. Of Chromatog. A*, 885, 153-193. [7] Dias R.F. and Freeman K. H. (1997) *Anal. Chem.* 69, 944-950.

## ISOTOPIC STUDY OF PRESOLAR GRAPHITE IN THE KFC1 SEPARATE FROM THE MURCHISON METEORITE.

S. Amari<sup>1</sup>, E. Zinner<sup>1</sup>, and R. S. Lewis<sup>2</sup>. <sup>1</sup>Laboratory for Space Sciences and the Physics Department, Washington University, St. Louis, MO 63130, USA (sa@wuphys.wustl.edu), <sup>2</sup>Enrico Fermi Institute, University of Chicago, Chicago, IL 60637, USA.

**Introduction and Experimental:** Graphite grains from the KFC1 separate (2.15-2.20g/cm<sup>3</sup>) extracted from the Murchison meteorite [1] are isotopically distinct from those of the other separates. Most notably, the *s*-process Kr isotopic ratios inferred from measurements on bulk samples indicate that KFC1 grains formed in low-metallicity asymptotic giant branch (AGB) stars ( $Z \leq 0.006$ ) [2]. We report isotopic analyses of graphite grains from the KFC1 separate. This is part of a continuing study of presolar graphite with a range of densities (1.65-2.20g/cm<sup>3</sup>). First, carbon grains on the KFC1d mount were documented with the SEM. Then, by the NanoSIMS [3], C and Si isotopic ratios of 86 grains were analyzed in multi-detection mode followed by Ti isotopic analysis in combined analysis mode, which utilizes multi-detection and magnetic peak jumping. <sup>50</sup>Ti was not determined because of large <sup>50</sup>Cr interference. Due to very low Ti concentrations, we analyzed only 28 grains. We include the unpublished data on eleven KFC1 grains obtained with the CAMECA-IMS3f in the following discussion.

**Discussion:** In a Si-three-isotope -value plot, 35 grains that exhibit an anomaly in either their Si or Ti isotopic ratios ( $>2\sigma$ ) lie on a straight line with a slope of  $0.56 \pm 0.05$  and an intercept of  $-31.1 \pm 5.5\text{‰}$ . This linear correlation can be explained by progressive alteration of the Si isotopic ratios in the envelope of AGB stars during the third dredge-up [4]. Titanium isotopic anomalies in 9 grains are characterized by excesses in <sup>46</sup>Ti and <sup>49</sup>Ti relative to <sup>48</sup>Ti, which is also expected as a result of neutron capture in the He intershell during the third dredge-up. The <sup>49</sup>Ti/<sup>48</sup>Ti ratios are as high as 5 times solar.

Another presolar grain type that is believed to have formed in low-metallicity AGB stars is SiC of type Z [5]. The differences between KFC1 graphite and Z grains are (1) <sup>12</sup>C/<sup>13</sup>C ratios of the graphite are higher (up to 4064) than those of Z grains (30-100) (2) The average <sup>29</sup>Si/<sup>28</sup>Si of the KFC1 graphite ( $-30 \pm 132\text{‰}$ ) is higher than that of Z grains ( $-76 \pm 57\text{‰}$ ). (3) <sup>46</sup>Ti/<sup>48</sup>Ti and <sup>49</sup>Ti/<sup>48</sup>Ti ratios of the graphite are much higher than the solar ratios, whereas those of the two Z grains measured for Ti isotopes are lower than the solar ratios [6]. The first observation indicates that the parent stars of Z grains had experienced cool bottom processing, which decreases <sup>12</sup>C/<sup>13</sup>C ratios in the envelope [7, 8], while the parent stars of the KFC1 graphite had not, suggesting that the latter have higher mass ( $>3M_{\text{sun}}$ ). The pronounced Ti excesses in the graphite agree with this hypothesis because final Ti isotopic ratios at the end of the third dredge-up are expected to increase with the mass of AGB stars [9]. The higher average <sup>29</sup>Si/<sup>28</sup>Si value of the graphite indicates higher metallicity of the parent stars of the graphite than of the parent stars of Z grains.

**References:** [1] Amari S. et al. 1994. *GCA* 58:459-470. [2] Amari S. et al. 1995. *GCA* 59:1411-1426. [3] Stadermann F. J. et al. 1999. LPS XXX, Abstract #1407. [4] Lugardo M. et al. 1999. *ApJ* 527:369-394. [5] Hoppe P. et al. 1997. *ApJ* 487:L101-L104. [6] Amari S. et al. 2003. *Meteorit. Planet. Sci.* 38:A66. [7] Charbonnel C. 1995. *ApJ* 453:L41-L44. [8] Wasserburg G. J. et al. 1995. *ApJ* 447:L37-L40. [9] Amari S. et al. 2001. *ApJ* 546:248-266.

## THE POTY QUARRY CONGLOMERATIC BED: THE RECORD OF A TSUNAMI TRIGGERED BY AN IMPACT?

J. A. Barbosa<sup>1</sup> and V. H. Neumann<sup>2</sup>. <sup>1</sup>PPGEO-UFPE, Av. Acadêmico Hélio Ramos, s/n, Cid. Univ. 50740-530. E-mail: barboant@hotmail.com., <sup>2</sup>DGEO-UFPE, Av. Acadêmico Hélio Ramos, s/n, Cid. Univ. 50740-530. E-mail: neumann@ufpe.br.

**Introduction:** The existence of a conglomeratic bed which separates the Cretaceous and Tertiary sedimentary units in the Poty quarry in the state of Pernambuco, Brasil. This conglomeratic bed was argued by Albertão and Martins Jr. [1], as a possible tsunami sedimentary record triggered by a Cretaceous-Tertiary impact. The recognition of this record was reinforced by the iridium anomaly that was found over the conglomeratic bed. In this opportunity we present petrographic and stratigraphic aspects, relative to the basin general context, which attempt to confirming the unique nature of this record, focusing the hypothesis of a fast and high energy event that strikes the basin, in this time.

**Results:** The sedimentary record is exposed in two places, along the Paraíba Marginal Basin, Northeast Brasil. The first observation is the extensive range of the record. The two outcrops sites are separated by 30km. Despite the distance, the record in both outcrops are very similar, with the same characteristics: a sharp-base erosional contact, a finning upward of intraclasts and the same textural aspects of the reworked material.

The observation of the stratigraphy along some sections covering the whole basin, revealed the absence of other beds with the same characteristics. The general bedding of the carbonate succession shows a very regular and aggradational platform. The absence of mass flows or tectonic activity invalidates the possibility of some type of debris flow. The lateral regularity of the conglomeratic bed is notable, and could indicate the occurrence of an extensive and regular episode, as a large wave, which instantly deposited a very regular bed (60cm thickness) over an area of at least 30km. The petrographic details obtained by samples of both outcrops reveals the reworking of carbonate fragments, and the mixing of eroded bioclasts of lower beds. Petrography of sampled outcrops and sedimentological studies of the conglomeratic bed, show that the event reach, and generated similar features over a relative marine open shelf in the southern area of the basin, and in a shallow northern area (stipulating that the separated outcrops recorded the effects of the same event).

**Conclusion:** The occurrence of a conglomeratic bed, deposited by a high energy event, with characteristics which made it a unique record in all the carbonate succession, is not a coincidence. Also, considering that over this bed occur an iridium anomaly, turn it an extraordinary evidencee. A possible tsunami could be generated by an earthquake or an impact. The lack of coeval tectonic evidences along the carbonate deposition disable the earthquake hypothesis. The possibility of a debris flow generated origin also is discarded by the stratigraphic and sedimentological observations, as we interpreted. So, the tsunami hypothesis is accepted as the most probable, regarding our sedimentological and stratigraphical data interpretation.

**References:** [1] Albertão, G. A. and Martins Jr, P. P. 1996. A possible tsunami deposit at the Cretaceous-Tertiary Boundary in Pernambuco, Northeastern Brazil. *Sedimentary Geology*. 104: 189-201.

### What does the CM chondrite Mineralogic Alteration Index really mean?

G.K. Benedix<sup>1</sup> and P.A. Bland<sup>2</sup>. <sup>1</sup>Dept. of Earth and Planetary Sciences, Washington University, St. Louis, MO, 63130-4899 E-mail: [gretchen@levee.wustl.edu](mailto:gretchen@levee.wustl.edu). <sup>2</sup>Dept. of Earth Science and Engineering, Imperial College, London SW7 2AZ, UK.

**Introduction:** CM chondrites contain minerals that formed by interaction between liquid water and anhydrous minerals [1]. How this process progressed on the parent body is important for understanding how to unravel the effects of aqueous alteration in these meteorites. Studies undertaken to qualify [1] and quantify [2] the extent of alteration found in the CMs resulted in a mineralogic alteration index (MAI) [2]. The MAI is a numerical representation of the  $\text{Fe}^{3+}/\text{Si}$  ratio in matrix phyllosilicates in CM meteorite falls. It has been found to correlate with carbonate [3] and sulfate [4] oxygen isotopic composition. One key question has been determination of the extent of terrestrial contamination within these meteorites.

**Discussion and Implications:** Figure 1 is a plot of MAI vs Year of Fall [5] for all the CM chondrites for which an MAI was determined [2]. MAI has a strong positive correlation with Year of Fall ( $R^2 = 0.93$ ); that is, the more altered meteorites are older. There is no such systematic correlation between Year of Fall and matrix or bulk  $\Delta^{17}\text{O}$ ,  $\delta^{18}\text{O}$  [6], water content or  $\delta\text{D}$  [7]. Although not as robust, a correlation also exists between Year of Fall and  $\Delta^{17}\text{O}$  in sulfate and carbonate, two minerals that are susceptible to interaction with liquid water. The fact that MAI and carbonate and sulfate  $\Delta^{17}\text{O}$  track with Year of Fall indicates that interaction with the terrestrial atmosphere may take place even if the meteorite is recovered immediately after its fall. The MAI may be providing a measure of terrestrial contamination.

**References:** [1] McSween H.Y. 1979 *Geochim. Cosmochim. Acta*. 43:1761-1770. [2] Browning L.B. et al. 1996 *Geochim. Cosmochim. Acta*. 60:2621-2633. [3] Benedix et al. 2003 *Geochim. Cosmochim. Acta* 67:1577-1588. [4] Airieau S. et al. 2001. Abstract #1744 32<sup>nd</sup> Lunar Planet. Sci. Conf. [5] Grady M.M. 2000. Catalogue of Meteorites. [6] Clayton R.N. and Mayeda T. 1999. *Geochim. Cosmochim. Acta*. 63:2089-2104. [7] Eiler J.M. and Kitchin N. 2004. *Geochim. Cosmochim. Acta*. 68:1395-1411.

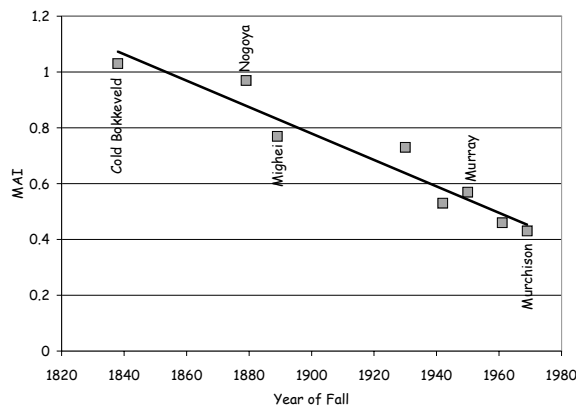


Figure 1. Mineralogic Alteration Index vs Year of Fall of CM chondrites. The line has a correlation coefficient of 0.93. The five most studied CM chondrites are labeled in the figure.

## EXPLORING THE POSSIBLE CONNECTION BETWEEN ORDINARY CHONDRITES AND PRIMITIVE ACHON- DRITES.

G.K. Benedix<sup>1</sup>, R. Ford<sup>2</sup>, T.J. McCoy<sup>3</sup>, T. Rushmer<sup>2</sup> and C.M. Corrigan<sup>3</sup>. <sup>1</sup>Dept. of Earth and Planetary Sciences, Washington University, Campus Box 1169, St. Louis, MO. 63130-4899 E-mail: gretchen@levee.wustl.edu. <sup>2</sup>University of Vermont, Dept. of Geology, Burlington, VT 05405. <sup>3</sup>Dept. of Mineral Sciences, Smithsonian Institution, Washington, DC. 20560-0119.

**Introduction:** Primitive achondrites are meteorites with chondritic bulk compositions, but non-chondritic textures [1]. Because their original chondritic textures have been erased, one important issue in the study of these groups is their origin [e.g. 2]. Most primitive achondrite groups have mineral compositions more reduced than ordinary chondrites, but more oxidized than enstatite chondrites [3]. Thus the question has been raised: Are their precursors a type of chondritic meteorite unknown in the world's collections or did these meteorites form by heating ordinary chondrites under reducing conditions? If the latter, this would imply changes during heating and partial melting so altered the primitive achondrites that they are not easily linked to their chondritic precursors. To test these ideas, we compare general properties of reduced primitive achondrites, focusing specifically on the winonaites/IAB group, and H-type ordinary chondrites. We illustrate, using results of heating experiments on ordinary chondrites [4], that initial composition plays a vital role.

**Discussion and Implications:** The most obvious difference between Win/IAB and H ordinary chondrites (Table 1) is oxidation state. Compositions of olivine, opx, chromite and troilite all point to Win/IAB being more reduced than H chondrites. Recent experiments [4] heated the H-chondrite Kernouvé at temperatures and under oxygen fugacities appropriate to Win/IAB [5]. While olivine and chromite exhibit evidence of reduction under these conditions, opx exhibits no change or a slight increase in Fs value with temperature. In troilite, Cr increases while Fe/S decreases with temperature. The results of the experiments indicate that in order to form the compositions seen in Win/IAB from an H-chondrite precursor, high peak-heating temperatures (in excess of 1200°C) are required. This is inconsistent with the textures and compositions seen in the Win/IAB. Thus, it appears improbable that Win/IAB formed by heating of a precursor assemblage similar to H chondrites, consistent with marked differences in oxygen isotopic composition [6].

**References:** [1] Prinz M. et al. 1983. 14<sup>th</sup> Lunar Planet. Sci. Conf. pp. 616-617. [2] Benedix G.K. et al. 1998. *GCA* 62:2535-2553. [3] Ford R. et al. 2003. Abstract #1713. 34<sup>th</sup> Lunar Planet. Sci. Conf. [4] Ford R. et al. 2004. Abstract #1095. 35<sup>th</sup> Lunar Planet. Sci. Conf. [5] Benedix G.K. et al. (2003) *MAPS* 38:A70. [6] Clayton R.N. and Mayeda T. 1996. *GCA* 60:1999-2018. [7] Mittlefehldt D.W. et al. (1998) Ch. 4, In Planetary Materials MSA Vol. 36. [8] Bunch T.E. et al. (1970) *Contrib. Min. Pet.* 25:297-340. [9] Gomes C.B. and Keil K. 1980. *Brazilian Stone Meteorites*. [10] Bunch T.E. et al. 1967. *GCA* 31:1569-1582.

Table 1. General properties of Win/IAB and H-chondrites.

Mineral		Win/IAB	H-chondrite
Olivine	Fa (mol%)	1 – 8 [2,5,8]	16.9 – 20.4 [9]
Opx	Fs (mol%)	1 – 8 [2,5,8]	15.7 - 18.1 [9]
Chromite	Cr/Cr+Al	0.9 - 1.0 [7,8]	0.85 [10]
Chromite	Fe/Fe+Mg	0.4 - 0.6 [7,8]	0.85 [10]
Chromite	MgO (wt%)	6-12 [7,8]	2.66 [9]
Troilite	Cr (wt%)	~0.4 [7,8]	BDL*

## ABUNDANCE AND MEANING OF REGOLITH BRECCIAS AMONG METEORITES.

A. Bischoff<sup>1</sup> and L. Schultz<sup>2</sup>. <sup>1</sup>Institut für Planetologie, Wilhelm-Klemm-Str. 10, 48149 Münster, Germany. E-mail: bischofa@nwz.uni-muenster.de. <sup>2</sup>Max-Planck-Institut für Chemie, Postfach 3060, 55020 Mainz, Germany.

**Introduction:** The study of meteoritic breccias contributes significantly to our understanding of early solar system processes of accretion, differentiation, and surface (regolith) evolution, and also provides unique information about the primordial, chemical and mineralogical characteristics of the accreted components themselves.

**Discussion:** Breccia-producing impacts took place prior to, simultaneously with, and after accretion and early differentiation of the parent bodies; impact metamorphism is an ongoing process producing not only gas-containing regolith, but also gas-poor fragmental breccias. Considering mineralogy and texture of breccias of various meteorite groups and the presence of incorporated solar particles (e.g., solar gases; Tab. 1), it may be possible to decide, if breccias result from cratering processes on a parent body without total destruction (*à la moon*), or from complete destruction of precursor parent bodies and formation of a new (second generation) body from which the meteorites derive.

**Table 1:** Percentage of solar gas containing meteorites. It is uncertain that some CV chondrites are true solar gas-rich regolith breccias (); some uncertainties also exist for the primitive achondrites; (a) No. of meteorites considered; (b) No. of meteorites with solar gases.

Chon.	(a)	(b)	%	Achon.	(a)	(b)	%
CI	6	6	100 %	Acap	12	0	0 %
CM	19	19	100 %	Win	2	0	0 %
CR	5	5	100 %	Lod	9	0	0 %
CO	21	0	0 %	Brach	7	0	0 %
CV	29	(5)	17.2 %	Aub	20	6	30.0 %
CK	21	0	0 %	How	21	8	38.1 %
CH	7	5	71.4 %	Euc	73	0	0 %
H	626	96	15.3 %	Dio	30	0	0 %
L	405	12	3.0 %	Ure	25	3	12.0 %
LL	110	6	5.5 %				
R	23	11	47.8 %				
E	73	7	9.6 %				

Often meteoritic breccias appear to result from impact cratering and mixing on a parent body without total destruction. This is probably the case for most ordinary, R-, and E-chondrite (regolith) breccias and achondritic breccias. Many of these breccias usually consist of a mixture of cognate clasts. For regolith breccias of most carbonaceous chondrites (CC) the situation is different. It is suggested that many breccias (e.g., from CM, CH, perhaps CI, CR) result from mixing of fragments after total destruction of (a) precursor parent bod(y)ies. Dark inclusions in CR and CH chondrites are excellent witnesses to document formation of the final parent body by secondary accretion. It is also suggested that most solar gases were incorporated into rock components prior to secondary accretion (exception: CM-chondrites). Main irradiation of CC components may have occurred (a) prior to primary accretion or (b) mineral or lithic fragments of destroyed bodies were irradiated prior to formation of the final parent body.

## THE PRODUCTION RATE OF SMALL CRATERS ON EARTH, AND THE EXPECTED CRATER POPULATION IN SOUTH AMERICA.

P.A. Bland<sup>1</sup>, N.A. Artemieva<sup>2</sup> and C.R. de Souza Filho<sup>3</sup>. <sup>1</sup>Dept. Earth Sci. & Eng., Imperial College, London SW7 2AZ, UK. E-mail: [p.a.bland@imperial.ac.uk](mailto:p.a.bland@imperial.ac.uk). <sup>2</sup>Inst. Dyn. Geospheres, Leninsky Pr., 38, Bldg.6, 119334, Moscow, Russia. <sup>3</sup>Instituto de Geociências, Universidade Estadual de Campinas, Campinas, Brazil.

**Introduction:** The craters preserved on the lunar mare provide a record of the rate of impacts and the impactor size distribution, over a mass range of  $\sim 10\text{-}10^{16}\text{kg}$ , for the 3.2-3.5Ga since the mare basalts were emplaced [1]. Constructing a similar curve for number of impacts over a given mass at the Earth's surface is complicated: the atmosphere disrupts meteoroids [2], and craters are removed by erosion and tectonism, or infilled. Since the terrestrial small crater record is incomplete, we chose to scale the known impact rate at the upper atmosphere to a flux at the surface by modelling how a given bolide behaves in the atmosphere.

**Methodology:** Most semianalytical approaches have considered impactors as strengthless liquid-like objects: so-called 'pancake' models, in which clouds of fragments are modelled as a continuous, lower-density, deformed impactor [2-4]. Unfortunately, these models are not capable of reproducing the cratering behaviour of fragmented asteroids. In contrast, Artemieva and co-workers [6-8] have developed a model that calculates motion, aerodynamic loading, and ablation, for each individual particle or fragment in a disrupted impactor. This approach allows us to predict a mass- velocity-distribution at the Earth's surface for a given impactor at the top of the atmosphere. The flux at the upper atmosphere has recently been constrained over a large portion of the mass range [9-16]. Our modelling data allows the flux curve for the upper atmosphere to be scaled to an impact rate at the Earth's surface, for objects from meteorites to 1km asteroids [17].

**Discussion:** Based on our calculated surface flux curve, we estimate that over the last 100Ma the continent of South America has experienced impacts producing  $\sim 18$  craters  $>10\text{km}$ , of which 12 would be  $>20\text{km}$ , and 1  $\sim 75\text{km}$ . Over a 1Ma period we would expect a single 1km crater, and  $\sim 200$  Campo del Cielo events.

The number of confirmed craters in Brazil (Araguainha, Serra da Cangalha, Riachão, Vargeão) is much lower than we would expect given the large area of the country, and the area and age of geologically stable target. It is interesting that the size-frequency distribution of possible craters derived from recent remote sensing data is a very close match to the expected population, given estimated impact rate, and the area and age of Brazilian basins.

**References:** [1] Hartmann W.K. *et al.* (1981) in *Basaltic Volcanism on the Terrestrial Planets* (Pergamon Press, New York), 1050. [2] Melosh H.J. (1981) in *Multi-Ring Basins* (Pergamon Press, New York), 29. [3] Chyba C.F. *et al.* (1993) *Nature* 361, 40. [4] Hills J.G., Goda M.P. (1993) *Astron. J.* 105, 1114. [5] Artemieva N.A., Shuvalov V.V., *Shock Waves* 5, 359 (1996). [6] Artemieva N.A., Shuvalov V.V. (2001) *J. Geophys. Res.* 106, 3297. [7] Shuvalov V.V. *et al.* (2000) *SSR* 34, 49. [8] Halliday I., Griffin A.A., Blackwell A.T. (1996) *MAPS* 31, 185. [9] Nemtchinov I.V. *et al.* (1997) *Icarus* 130, 259. [10] Brown P. *et al.* (2002) *Nature* 420, 294. [11] ReVelle D.O. (1997) *Ann. NY Acad. Sci.* 822, 284. [12] Morbidelli A. *et al.* (2002) *Icarus* 158, 329. [13] Rabinowitz D. *et al.* (2000) *Nature* 403, 165. [14] Stuart J.S. (2001) *Science* 294, 1691. [15] Harris A.W. (2004) in *Proc. Asteroids, Comets, Meteors 2002*. [16] Bland P.A., Artemieva N.A. (2003) *Nature* 424, 288.

## MAPS OF ELEMENTAL ABUNDANCES ON THE SURFACE OF MARS.

W. Boynton<sup>1</sup>, D. Janes<sup>1</sup>, K. Kerry<sup>1</sup>, K. Kim<sup>2</sup>, R. Reedy<sup>2</sup>, L. Evans<sup>3</sup>, R. Starr<sup>3</sup>, D. Drake<sup>4</sup>, J. Taylor<sup>5</sup>, and H. Wänke<sup>6</sup>. <sup>1</sup>Univ. Arizona, <sup>2</sup>Univ. New Mexico, <sup>3</sup>Goddard, <sup>4</sup>TechSource, <sup>5</sup>Univ. Hawaii, <sup>6</sup>MPI-Mainz.

**Introduction:** In this work we present maps of K, Th, Si, Fe, Cl, and H abundance distribution over the low and middle latitudes of Mars. The distribution of the elements in the polar regions are difficult to map quantitatively, as the very high ice content both dilutes the elemental abundance as well as significantly alters the flux of thermal neutrons, which are the excitation source of all but the first two elements in the list above.

**Data Processing:** Maps of the two radioactive elements, K and Th, are made directly from their decay constants and the observed gamma-ray flux. The abundances of the other four elements, which produce gamma rays following the capture of thermal neutrons, are first calculated as element/Si ratios, which removes the uncertainties in the flux of thermal neutrons at the surface. The ratios are converted to elemental abundances by multiplying by Si abundances determined via fast neutron interactions. (The fast neutron flux at the surface can be estimated from the orbital measurements.) The Si map is normalized to a Si abundance of 21.1% at the location of the Mars Pathfinder landing site

**Results:** The data show that Mars has a significant contrast in elemental composition over different regions.

*Silicon.* Silicon shows only modest variation over the surface. It ranges from about 18% Si (+/- 0.4%) to 23% Si (+/- 0.8%) with the lower values being associated with the Tharsis volcanoes and other basaltic lava flows.

*Iron.* Iron shows a much greater than expected range in composition. The northern lowlands have higher iron content; most areas are in the range of 11% to 14.5% Fe, which overlaps the low end of the SNC meteorite range. The highlands, on the other hand, have much lower Fe content; most areas are in the range of 8 to 11% Fe, which is much lower than in the SNC meteorites

*Hydrogen.* Hydrogen shows a wide variation in abundance in the low to middle latitudes. Excluding the regions where H increases toward the poles due to sub-surface ice, we see a variation from about 0.85% to 7.5% H<sub>2</sub>O. The areas of greatest enrichment are the dusty region of Arabia as well as the region antipodal to Arabia.

*Chlorine.* Chlorine also shows a wide range in composition. There is a region of remarkably high Cl content, up to 1.1% Cl, west of Tharsis in a region called Madusa Fossae. This region is thought to be an ignimbrite, or ash-fall deposit, and the high Cl abundance is probably associated with this formation. It is remarkable in that even though this region is being eroded by winds, the high Cl is confined to this one area. The Cl distribution over the remaining area shows a correlation with the distribution of H, suggesting both are associated with weathering.

*Potassium.* Potassium is strongly enriched in the region of Mars that corresponds to the TES surface type-2 region (andesite or weathered basalt) and is much less abundant elsewhere. The lowest K abundance, around 0.25 % K occurs in the regions of basaltic lava flows.

*Thorium.* Thorium shows a similar distribution to K and is strongly correlated with it. The K/Th ratio, however, is not constant, as normally expected from igneous processes, suggesting that weathering may be at least partly responsible for the distribution of these elements.

**CATHODOLUMINESCENCE STUDY OF ALBITIC FELDSPARS AND CA-PHOSPHATES IN TYPE 4-6 ORDINARY CHONDRITES.** F. Brandstätter. Naturhistorisches Museum, Postfach 417, A-1014 Vienna, Austria. E-mail: franz.brandstaetter@nhm-wien.ac.at.

**Introduction:** Many mineral phases which occur in meteorites show cathodoluminescence (CL) [1]. CL properties have been investigated in different ways ranging from bulk CL spectroscopy (CLS) of cm-sized areas to CLS of  $\mu\text{m}$ -sized single mineral phases. Recent examples are the use of CL color indices as a parameter for petrologic changes in meteorites [2] and CLS of experimentally shock-metamorphosed quartzite [3]. Here, I report on the preliminary results of CLS of albitic feldspars (60 grains), chlorapatite (11 grains), and whitlockite (8 grains) from 15 type 4-6 ordinary chondrites (including H, L and LL).

**Experimental:** CL spectra were acquired with an Oxford MonoCL2 system attached to a JEOL JSM 6400 SEM operated at 15 kV accelerating voltage and 2.2 nA beam current. All spectra were recorded in the range of 200-800 nm with 2 nm wavelength steps. Scanned areas of feldspars and phosphates were about 100  $\mu\text{m}^2$  and 400  $\mu\text{m}^2$ , respectively. The selected areas were also analyzed by analytical SEM for major element compositions and to check for possible interference with adjacent mineral phases.

**Results and discussion:** *Feldspars* are albitic plagioclases with end member compositions within the range  $\text{An}_{10-12}\text{Ab}_{82-86}\text{Or}_{4-6}$  as compiled for equilibrated OCs [4]. All recorded CL spectra are dominated by one broad peak in the blue region centered around 430-440 nm. This peak has an asymmetric shape with a FWHM in the range of 110-140 nm. The blue emission occurring in almost all feldspars has been related to structural defects [5]. Blue CL with one broad peak centered around 430 nm has also been reported for terrestrial alkali feldspars [6]. However, no correlation between CL properties of feldspar grains and their host meteorite (type or chondrite group) could be observed in this study.

*Chlorapatites* typically show little variation in their major element composition [4] containing 5.0-5.5 wt% chlorine. CL spectra exhibit two broad emission peaks centered around 374 nm and 580 nm. In most cases the relative intensity ratios of these two peaks are different for different grains. These observed variation in CL intensity of chlorapatite could be related to the crystal orientation dependence of CL in apatite crystals [7]. However, the overall shape of the spectra is most likely controlled by the presence of component CL bands of REE activators [8].

*Whitlockites* typically contain significant amounts of  $\text{Na}_2\text{O}$  (2.4-3.1 wt%) and  $\text{MgO}$  (3.8-4.4 wt%). CL spectra exhibit distinct peaks centered around 348 and 365 (double peak), 481, 572 and 647 nm. In contrast to the chlorapatites, the overall shape of the CL spectra of all whitlockites investigated so far is roughly the same. Therefore, CLS could be used to identify whitlockite in meteorites.

**References:** [1] Steele I. A. 1989. 20th Lunar & Planetary Science Conference. pp. 1052-1053. [2] Meier A. et al. 2003. Abstract #1037. 34th Lunar & Planetary Science Conference. [3] Gucsik A. et al. 2003. *Meteoritics & Planetary Science* 38: 1187-1197. [4] Brearley A. J. and Jones R. H. 1998. In: *Planetary Materials* (ed. Papike J. J.). Rev. Mineral. 36. Mineral. Soc. America:3/1-398. [5] Götz J. et al. 2000. In: *Cathodoluminescence in Geosciences* (eds. Pagel M. et al.). Springer N. Y.: 245-270. [6] Finch A. A. and Klein J. 1999. *Contributions to Mineralogy and Petrology* 135: 234-243. [7] Barbarand J. and Pagel M. 2001. *American Mineralogist* 86: 473-484. [8] Blanc P. et al. 2000. In: *Cathodoluminescence in Geosciences* (eds. Pagel M. et al.). Springer N. Y.: 127-160.

## PETROGRAPHIC CLASSIFICATION AND CHONDRULE TEXTURES OF FOSSIL METEORITES FROM SOUTHERN SWEDEN.

J. C. Bridges<sup>1</sup>, B. Schmitz<sup>2</sup> and R. Hutchison<sup>3</sup> <sup>1</sup>PSSRI, Open University, Milton Keynes MK7 6AA, UK. j.bridges@open.ac.uk.

<sup>2</sup>Department of Geology, University of Lund, Lund, SE-22362, Sweden. <sup>3</sup>Department of Mineralogy, Natural History Museum, London SW7 5BD, UK.

Over 12 separate fossil meteorite falls have been identified in the mid-Ordovician limestone of Thorsberg, southern Sweden [1, 2]. Their affinity to L chondrites has been suggested through chemical analyses of relict chromite grains. Here we start extending the classification of the samples to provide petrographic types.

In order to do this we have determined the abundance and grain size of chromite grains within fossil meteorites and compared the results with similar counts on recent meteorites. The counts and measurements on the fossil meteorite blocks were done with a low-vacuum chamber analytical SEM. We have also recorded the relict chondrule textures.

Chromite is the only mineral phase that has been preserved with its initial meteoritic chemistry during the diagenesis of the fossil meteorites. However in some samples there has also been near perfect pseudomorphing of chondrule textures, and where possible this has also been used for determining petrographic type. Ordinary chondrites contain progressively higher abundance of coarser sized chromite grains with increasing petrographic type. Three of the recent meteorites of lower petrographic type used in our comparative study are Parnallee (LL3.6), Floyd (L4) and Julesburg (L3.7). Higher petrographic type OCs studied include Dhurmsala (LL6) and New Concord (L6).

Julesburg has a mean chromite grain size of 10 m, range 5-50 m; Floyd has mean = 50 m, range = 10-150 m. On the basis of chromite measurements we suggest the following petrographic types: Ark032 (mean = 50 m) type 4 or 5; Ark003 (mean = 90 m) type 5 or 6; Ark010 (mean = 20 m) type 3; Skj001 (mean = 35 m) type 4 or 5; Sext001 (mean = 40 m) type 4 or 5. See [1] for meteorite names and distribution. The classification of Ark010 as a relict L3 chondrite is supported by its preserved chondrule outlines and textures. Chondrule textures in the samples (pseudomorphed by carbonate and barytes) include radiating-pyroxene, porphyritic and barred textures.

Our results suggest that the Middle Ordovician meteorite falls preserved in southern Sweden consist of a range of petrographic types from 3 to 5/6.

**References:** [1] Schmitz B. et al. 2001. *Earth Planet. Sci. Lett.* 194:1-15. [2] Schmitz B. et al. 2001. *Meteoritics & Planetary Science* 36: A183.

## OLIVINE DECOMPOSITION FEATURES IN THE Y000593 AND NWA998 NAKHLITES.

J. C. Bridges<sup>1</sup>, P. H. Warren<sup>2</sup> and M. R. Lee<sup>3</sup> <sup>1</sup>PSSRI, Open University, Milton Keynes MK7 6AA, UK. j.bridges@open.ac.uk.

<sup>2</sup>Institute of Geophysics, University of California, Los Angeles, CA 90095-1567 USA. <sup>3</sup>Division of Earth Sciences, University of Glasgow, Glasgow G12 8QQ, UK.

**Introduction:** Olivine grains within the 6 nakhlites show signs of partial breakdown both from limited exsolution and through a later, low-temperature, rapid brine-evaporation event associated with fracture-filling siderite-clay mixes e.g. [1,2]. We report results of EPMA and analytical-TEM with focused ion beam sample preparation studies of Y000593 and NWA998 in order to characterise olivine-decomposition in the nakhlites.

**Results:** We have identified exsolution lamellae composed mainly of stoichiometric Ca-rich olivine within Y000593 olivine grains. They have a similar dark brown, oxidised appearance in ppl as augite-magnetite symplectites in Nakhla and are typically 50 x 5 m. Their compositions are Mg\* = 28-33, Ca/(Ca+Mg+Fe) = 0.16-0.28 with CaO = 9-16 wt%. The CaO contents of the surrounding olivine are 0.6 wt%. However, some exsolution lamellae in Y000593 are composed of augite (En29-39 Fs23-33 Wo38-40).

The carbonate-clay intergrowths in Y000593 and NWA998 are too fine-grained to allow for pure carbonate analyses to be determined by EPMA. Therefore we determined a range of clay-carbonate mix compositions and by extrapolation the 0 wt% SiO<sub>2</sub> end-member was taken as the carbonate composition. The Y000593 carbonate is Cc 7.3%, Rh 1.9%, Mg 13.9%, Sd 76.9%. This is similar – although in the lower range of Mn contents – to that described in Nakhla and Governador Valadares (GV) [1]. Siderite in Nakhla [1] has an overall range of Cc 0.1-5.7%, Rh 1.0-39.9%, Mg 2.0-40.9%, Sd 23.2-87.0%. Both GV and Nakhla contain carbonate and related minerals within interstitial, mesostasis areas in addition to fractures within olivine [1]. We have found no interstitial siderite in Y000593 or NWA998.

Two <20 m samples were separated from siderite-clay veins in Y000593 by a focused ion beam technique [3]. ATEM analyses of the samples confirm the presence of crystalline siderite. They reveal the amorphous nature both of the Fe-rich clay and also some of the olivine immediately surrounding the veins in zones <5 m wide. Whether this is related to fracturing, limited alteration by the brine or are an artifact of the ion beam is not yet clear.

**Discussion:** Symplectite exsolutions described in Nakhla are considered to be formed from the breakdown of Ca-rich olivine to augite and magnetite [2]. Our discovery of Ca-rich olivine exsolutions in Y000593 may be due to fast cooling in an upper part of the nakhlite cumulate pile as suggested by [4]. Initial REE data we are collecting e.g. [5] may be consistent with a slightly more evolved melt composition than Nakhla and we are exploring this question further. Siderite composition in Y000593 is consistent with the metastable carbonate compositions in nakhlites [1,6] formed through rapid evaporation of a brine.

**References:** [1] Bridges J. C. and Grady M. M. 2000. *Earth Planet. Sci. Lett.* 176, 267-279. [2] Mikouchi T. et al. 2000. *Meteoritics & Planetary Science* 35, 937-942. [3] Lee M. R. et al. 2003. *Mineralogical Magazine* 67, 581-592. [4] Mikouchi T. et al. 2003. *Antarct. Meteorite Res.* 16, 34-57. [5] Bridges J. C. et al. 2000. *Meteoritics & Planetary Science* 38, A119. [6] Bridges J. C. et al. 2001. *Space Science Reviews* 96, 365-392.

**AN ION PROBE STUDY OF THE SULPHUR ISOTOPIC COMPOSITION OF FE-NI SULPHIDES IN CM CARBONACEOUS CHONDRITES.** E. S. Bullock<sup>1</sup>, K. D. McKeegan<sup>2</sup>, M. Gounelle<sup>1,3</sup>, M. M. Grady<sup>1</sup>, S. S. Russell<sup>1</sup>, <sup>1</sup>Department of Mineralogy, The Natural History Museum, Cromwell Road, London, SW7 5BD UK; <sup>2</sup>Department of Earth and Space Sciences, UCLA, Los Angeles, CA 90095; <sup>3</sup>CSNSM, Université Paris 11, Bâtiment 104, 91 405 Orsay Campus, France. Email E.Bullock@nhm.ac.uk.

**Introduction:** The CM chondrites have endured variable degrees of aqueous alteration [1] which has changed their original mineralogy. A detailed study of the petrology and mineralogy of the sulphides in a suite of increasingly aqueously altered CMs, combined with sulphur isotope data measured *in situ*, can provide clues as to whether differences in the CM group are a result of different degrees of aqueous alteration, or whether they are the result of nebular heterogeneity.

**Previous studies:** A previous study of the sulphur isotopic values of chemically extracted Fe-Ni sulphides in 3 CM chondrites yielded values with up to 10‰ variation in  $\delta^{34}\text{S}_{\text{CDT}}$ , and 5‰ variation in  $\delta^{33}\text{S}_{\text{CDT}}$  [2]. Sulphur isotopes in Fe-Ni sulphides have been studied in two CM1 samples: an ion probe study of sulphides in the CM1 lithology in Kaidun [3,4] showed a range of  $\delta^{34}\text{S}_{\text{CDT}}$  values from -5.7‰ to +1.1‰, and an ion probe study of sulphides in the Antarctic CM1 ALH88045 [5], which gave  $\delta^{34}\text{S}_{\text{CDT}}$  values ranging from -1.7‰ to +1.8‰ and  $\delta^{33}\text{S}_{\text{CDT}}$  values of -0.8‰ to +1.0‰.

**Method:** One section from each of the following CM2s (listed in order of increasing alteration according to [1]) was studied: Bells, Murray, Mighei and Cold Bokkeveld. One section of the CM1 chondrite ALH88045 was also analysed. The isotopes  $^{32}\text{S}$ ,  $^{33}\text{S}$  and  $^{34}\text{S}$  were measured with the UCLA Cameca IMS 1270 in multicollector mode following the method outlined in [6]. Chemical compositional data for the sulphides were collected using the Cameca SX50 EMP at the Natural History Museum.

**Results and Discussion:** All of the grains studied in the CM chondrites were pyrrhotite or pentlandite, or a mixture of these two phases. All of the data points lie on the terrestrial mass-dependent fractionation line. The  $\delta^{34}\text{S}_{\text{CDT}}$  values for the CM2 chondrites range between -7.0‰ to +6.1‰, whilst  $\delta^{33}\text{S}_{\text{CDT}}$  vary between -3.5‰ to +3.4‰. The results obtained for the CM1 ALH88045 overlap those obtained previously by [5], with  $\delta^{34}\text{S}_{\text{CDT}}$  values from -2.9‰ to -0.4‰ and  $\delta^{33}\text{S}_{\text{CDT}}$  values between -1.4‰ and -0.2‰. There are no isotopic differences apparent between sulphide grains occurring in the matrix, and those that form chondrule rims. There was no progressive increase in the proportion of heavier isotopes with increasing alteration, as might be expected if sulphates were forming by alteration of sulphides and preferentially removing the lighter isotopes. This suggests that the S isotopic composition of the sulphides was not defined by progressive alteration on the parent body.

**References:** [1] Browning L. B. et al *Geochimica et Cosmochimica Acta* 60: 2621-2633. [2] Gao X. and Thiemans M. H. (1993) *Geochimica et Cosmochimica Acta* 57: 3159-3169 [3] McSween H. Y. et al (1996) 27<sup>th</sup> Lunar and Planetary Science Conference: 855-856. [4] McSween H. Y. et al (1997) *Meteoritics and Planetary Science* 32: 51-54. [5] Bullock E. S. et al (2003) *Meteoritics and Planetary Science* 38: A143 [6] Farquhar J. et al (2002) *Science* 298, 2369-2372.

## TWO LARGE MOROCCAN MESOSIDERITES: NWA 1817/1878/1979/2042 AND NWA 1827/1879/1882/1912/1951/1982/3055.

T. E. Bunch<sup>1</sup>, A. J. Irving<sup>2</sup>, J. H. Wittke<sup>1</sup> and S. M. Kuehner<sup>2</sup>,  
<sup>1</sup>Dept. of Geology, Northern Arizona University, Flagstaff,  
AZ 86011, <sup>2</sup>Dept. of Earth & Space Sciences, University of  
Washington, Seattle, WA 98195

**Discovery:** Two different, relatively large mesosiderites assignable to classes B and C [1] were found in Northwest Africa during 2003. Samples of both finds were distributed by various Moroccan dealers, but locations are not known. Portions of each heterogeneous meteorite have been studied in several laboratories and assigned different numbers [2]; we have examined most of the individual fresh samples.

**Samples:** The first group of specimens (Class B, coarse grained, with large spheroidal metal grains) includes NWA 1817 (*Hupé/Oakes*), NWA 1878 (*Hupé*), NWA 1979 (*Boswell*), NWA 2042 (*Gregory*), and other material with a total known weight of at least 6.4 kg. The second group of specimens (Class C, finer grained, heterogeneous, with large orthopyroxene and some plagioclase macrocrysts) includes NWA 1827 (*Oakes*), NWA 1879 (*Hupé*), probably NWA 1882 (*Ralew*), NWA 1912 (*Farmer*), NWA 1951 (*Moroccan Imports*), NWA 1982 (*Fectay*), NWA 3055 (*Anon.*), and other material with a total known weight of at least 26.4 kg. NWA 1645 (*Farmer*) [2] possibly also is paired with these.

**Petrography:** NWA 1817 and pairings consist of subequal amounts of metal and silicates in a coarse grained, unbreciated, plutonic igneous texture. The metal (about 40 vol.%) is concentrated in spheroidal clusters interspersed with more silicate-rich material, and consists mainly of kamacite with rounded taenite grains and rare schreibersite. The remainder consists mainly of orthopyroxene ( $\text{Fs}_{30-31}\text{Wo}_2$ ,  $\text{FeO}/\text{MnO} = 23.2\text{-}30.1$ ) with lesser amounts of anorthitic plagioclase ( $\text{An}_{90-93}$ ), silica polymorph, troilite, chromite and merrillite; rare angular olivine grains ( $\sim\text{Fa}_{40}$ ,  $\text{FeO}/\text{MnO} = 42.3$ ) and clasts of gabbroic eucrite and diogenite also are present. In contrast NWA 1827 and pairings, while also exhibiting igneous textures, are generally medium grained, but with distinctive large grains of glassy orthopyroxene. Orthopyroxene predominates in these samples, with about 10 vol.% metal (kamacite), troilite, chromite, merrillite, silica polymorph and sparse, large plagioclase grains ( $\text{An}_{89-95.5}$ ). Some large orthopyroxene macrocrysts (which may derive from diogenitic precursors) are more magnesian ( $\text{Fs}_{16.2}\text{Wo}_{0.8}$ ,  $\text{FeO}/\text{MnO} = 34.8$ ) than the predominant medium-sized orthopyroxene grains ( $\text{Fs}_{23-31}\text{Wo}_{2-3}$ ,  $\text{FeO}/\text{MnO} = 29.7\text{-}32.7$ ), which are more typical of mesosiderites. Some plagioclase-poor portions of these samples (such as NWA 1827, NWA 1982) could be misidentified as “metal-rich diogenite”.

**References:** [1] Hewins, R. (1988) *Meteoritics* 23, 123-129; [2] Russell, S. et al. (2004) *Meteorit. Bull.* 88.

**NEAR-INFRARED SPECTROSCOPY OF VESTOIDS**

T. H. Burbine,<sup>1</sup> T. J. McCoy,<sup>2</sup> J. M. Sunshine,<sup>3</sup> A. S. Rivkin,<sup>4</sup> and R. P. Binzel,<sup>4</sup> and S. J. Bus<sup>5</sup>. <sup>1</sup>Laboratory for Extraterrestrial Physics, NASA Goddard Space Flight Center, Greenbelt, MD 20771, USA. E-mail: tburbine@lepvax.gsfc.nasa.gov.

<sup>2</sup>Department of Mineral Sciences, National Museum of Natural History, Smithsonian Institution, Washington, DC 20560, USA.

<sup>3</sup>Science Applications International Corporation, Chantilly, VA 20151, USA. <sup>4</sup>Department of Earth, Atmospheric, and Planetary Sciences, Massachusetts Institute of Technology, Cambridge, MA 02139, USA. <sup>5</sup>University of Hawai'i, Institute for Astronomy, Hilo, HI 96720, USA

**Introduction:** Asteroid 4 Vesta is the most studied asteroid due to its large size (~500 km diameter) and its spectral resemblance to the HEDs (howardites, eucrites, and diogenites) [1]. A number of smaller ( $\leq$ 10 km diameter) objects (called Vestoids) have also been found [2, 3, 4] to have a spectral resemblance to the HEDs. The Vestoids have been found both inside and outside the dynamical boundaries defined for the Vesta family.

We have instituted a near-infrared spectral study of a number of Vestoids to determine their mineralogy. The goal of our study is better understand the compositional diversity of basaltic material on the scale of  $\sim$ 10 km.

**Telescopic Data:** Near-infrared telescopic data were obtained using SpeX [5], a low- to medium-resolution spectrograph at the NASA Infrared Telescopic Facility on Mauna Kea. Six different Vestoids (1906 Naeff, 2653 Principia, 2851 Harbin, 3782 Celle, 3869 Norton, and 4215 Kamo) were observed over the course of two nights. Also, a set of five to six solar-like stars were observed each night. Standard reduction techniques were used to reduce the spectra. Each asteroid's near-infrared reflectance spectrum is scaled to overlap its visible spectrum [6, 7], which results in wavelength coverage from  $\sim$ 0.4 to 2.5  $\mu$ m.

**Analysis:** The Vestoids all have distinctive absorption bands centered near 0.9 (Band I) and 1.9-2.0  $\mu$ m (Band II) due to pyroxene plus a shallow inflection centered near 1.2  $\mu$ m due to plagioclase. The wavelength position of the Band II center is a function [8] of the average pyroxene composition of the material with eucrites having Band II centers at longer wavelengths than the diogenites due to the more Ca-and Fe-rich nature of the eucritic pyroxenes. The Band II centers of the Vestoids are most consistent with those of polymict eucrites/howardites [3], implying appreciable amounts of diogenitic material on their surfaces.

**Conclusions:** Near-infrared reflectance spectra of these six Vestoids confirm the basaltic nature of their surfaces. Our future work will be to determine mineralogies of these objects.

**References:** [1] McCord T. B. et al. 1970. *Science* 168, 1445-1447. [2] Binzel R. P. and Xu S. 1993. *Science* 260, 186-191. [3] Burbine T. H. et al. 2001. *Meteoritics & Planetary Science* 36, 761-781. [4] Kelley M. S. et al. 2003. *Icarus* 165: 215-218. [5] Rayner J. T. et al. 2003. *Publications of the Astronomical Society of the Pacific* 115, 362-382. [6] Xu S. et al. 1995. *Icarus* 115, 1-35. [7] Bus S. J. and Binzel R. P. 2001. *Icarus* 158, 106-145. [8] Adam J. B. 1974. *Journal of Geophysical Research* 87, 4829-4836.

**Acknowledgements:** The data was obtained while T. H. Burbine and T. J. McCoy were visiting astronomers at the Infrared Telescope Facility, which is operated by the University of Hawaii under Cooperative Agreement no. NCC 5-538 with the National Aeronautics and Space Administration, Office of Space Science, Planetary Astronomy Program.

**NOBLE GASES FROM THE INTERSTELLAR MEDIUM  
TRAPPED ON THE MIR SPACE STATION AND  
ANALYZED BY IN VACUO ETCHING.**

H. Busemann<sup>1\*</sup>, F. Bühlert<sup>1</sup>, Y.N. Agafonov<sup>2</sup>, H. Baur<sup>3</sup>, P. Bochsler<sup>1</sup>, N.A. Eismont<sup>2</sup>, V.S. Heber<sup>1,3\*\*</sup>, R. Wieler<sup>3</sup> and G.N. Zastenker<sup>2</sup>. <sup>1</sup>Physikalisches Institut, University of Bern, Switzerland. <sup>2</sup>IKI, Russian Academy of Sciences, Moscow, Russia. <sup>3</sup>Earth Sciences, ETH Zurich, Switzerland. Present addresses: \*E-mail: busemann@dtm.ciw.edu. DTM, Carnegie Institution, Washington DC, USA. \*\*Earth Sciences, Open University, Milton Keynes, UK.

**Introduction:** The composition of the present interstellar medium (ISM) provides an important benchmark in cosmochemistry. It serves as a reference for galactic chemical evolution (GCE) models, solar mixing predictions and provides information for understanding Big Bang nucleosynthesis. The present-day ISM  ${}^3\text{He}$  abundance allows, combined with the protosolar  ${}^3\text{He}$ , deduced from the Jovian atmosphere or meteorites [1,2], tracing the GCE over the past 4.56 Ga.  ${}^3\text{He}/{}^4\text{He} = (2.5 \pm 0.6) \times 10^{-4}$  has been determined for the local ISM [3]. However, the uncertainty is too large to better constrain GCE models and - in combination with the present-day solar wind value - the protosolar D/H [4].

**Experiment:** The COLLISA experiment [*Collection of Inter-Stellar Atoms*, 5,6] sampled interstellar gas in Cu-Be foils covered with BeO and exposed to the flux of neutrals from the ISM on board the MIR space station. Stepwise heating extraction allowed the detection of interstellar  ${}^4\text{He}$  [6] and yielded  $({}^3\text{He}/{}^4\text{He})_{\text{ISM}} = (1.7 \pm 0.8) \times 10^{-4}$  [7], in agreement with the value for pickup ions observed with SWICS/Ulysses [3].

Further foils are currently analyzed by closed system stepwise etching at ETH Zurich [8]. This technique allows to efficiently separate implanted interstellar He and terrestrial tritogenic  ${}^3\text{He}$ , probably residing in the Cu-Be substrate, which had to be taken into account for the determination of interstellar  ${}^3\text{He}$  during stepwise heating [7].

**Results:** Offline tests suggest that HF acid vapor efficiently and uniformly etches BeO. The system blank (in  $10^{-14} \text{ cm}^3$  STP,  ${}^3\text{He} \sim 3$ ,  ${}^4\text{He} \sim 300$ ,  ${}^{20}\text{Ne} \sim 90$ ) is now sufficiently low to measure the exposed foils. Two unexposed foils (31 and  $50 \text{ cm}^2$ ) were etched online and yielded no significantly increased values relative to these blanks, implying that the tritogenic  ${}^3\text{He}$  ( $0.5-1 \text{ } 10^{-14} \text{ cm}^3/\text{cm}^2$  foil) indeed resides in deeper foil layers that are not affected by superficial etching. The analysis of a foil artificially irradiated with  ${}^3\text{He}$  and  ${}^{20}\text{Ne}$  at energies comparable to those of the ISM neutrals (25 eV/amu) showed that our protocol (10 steps 1-30 min, HF vapor at 20 °C) releases all trapped noble gases. Results of the ongoing etching experiment on foils exposed to the ISM (including a witness foil doped with terrestrial  ${}^3\text{He}$ ) will be presented. The expected concentrations of interstellar gas [3,6,7] in  $50 \text{ cm}^2$  of exposed foil are (in  $10^{-14} \text{ cm}^3$  STP)  ${}^3\text{He} \sim 25$ ,  ${}^4\text{He} \sim 200000$ ,  ${}^{20}\text{Ne} \sim 375$ .

**Acknowledgement:** This work was supported by the Swiss NSF. Technical support by U. Menet is gratefully acknowledged.

**References:** [1] Mahaffy P. R. et al. 2000. *JGR* 105:15061-15071. [2] Busemann H. et al. 2001. *Lunar Planet. Sci. Conf.* XXXII:#1598. [3] Gloeckler G. and Geiss J. 2001. *AIP Conf. Proc.* 598:281-289. [4] Geiss J. and Gloeckler G. 2002. *Space Sci. Rev.* 105:3-18. [5] Zastenker G. N. et al. 2002. *Cosmic Research* 40:347-357. [6] Bühlert F. et al. 2000. *Astrophys. Space Sci.* 274:19-24. [7] Salerno E. et al. 2003. *Astrophys. J.* 585:840-849. [8] Busemann H. 2000. *Meteorit. Planet. Sci.* 35:949-973.

**CONSTANT SUNLIGHT AT THE LUNAR NORTH POLE.**

D. B. J. Bussey<sup>1</sup>, K. Fristad<sup>2</sup>, P. Schenk<sup>3</sup>, M. S. Robinson<sup>4</sup>, and P. D. Spudis<sup>1</sup>. <sup>1</sup>The Johns Hopkins University Applied Physics Laboratory, 11100 Johns Hopkins Road, MP3-E180, Laurel MD 20723 (ben.bussey@jhuapl.edu) <sup>2</sup>Macalester College, 1600 Grand Ave, Saint Paul MN 55105, <sup>3</sup>Lunar and Planetary Institute, Houston TX 77058. <sup>4</sup>Northwestern University, Lacy Hall 309, 1847 Sheridan Road, Evanston IL 60208,

**Introduction:** The existence of permanent sunlight in the lunar polar regions has important ramifications for long duration operations on the lunar surface. Regions which are permanently sunlit would not only have the availability of constant solar power generation but these areas would permit operations in a reasonably benign thermal environment. It has been modeled that the temperature of a permanently sunlit region close to a lunar pole would be 223 – 10 K [1].

**Clementine Data:** The Clementine spacecraft acquired images of each pole once every 10 hours for 71 days in 1994. These show how the lighting varies for a range of different insolation conditions. These data were collected during summer in the northern hemisphere.

*Quantitative illumination map.* Clementine UVVIS data have been used to produce the first quantitative illumination map of the lunar north pole region. This map shows the percentage of time that a point on the surface is illuminated during an entire day. An analysis of this map has identified four regions on the rim of Peary crater ( $88.6^{\circ}$  N  $33.0^{\circ}$  E, 73km) that were illuminated for an entire lunar day (708 hours)[2]. As these data were collected just after mid summer it is not possible to claim that they are permanently lit, however they do represent the most likely sites on the Moon that could be constantly sunlit.

*Qualitative study of expanded area.* Due to the technique used to produce the quantitative map, the spatial coverage of the map is limited to between  $1^{\circ}$  and  $1.5^{\circ}$  of the north pole. Examination of obliquely acquired data has expanded our knowledge of the illumination conditions near the pole by providing qualitative information on other regions that appear to receive large amounts of illumination. These data cover a greater distance over the pole, and therefore into the nominal “darkside”, thus showing topographically high regions that are tall enough to be in sunlight. We have identified three regions, between  $2^{\circ}$  and  $3^{\circ}$  from the pole which were illuminated. These occur on the rims of the impact craters Hermite, Rozhdestvensky, and Peary.

**Galileo:** Galileo acquired images of the lunar surface during its 2 lunar flybys. Some of these covered the north pole of the Moon. Whilst this only shows a snapshot of the illumination conditions in this area, it is of particular interest because the data were acquired during a different part of the year compared to the Clementine data. Specifically, it was Autumn in the northern hemisphere. A mosaic of Galileo SSI images shows that the northern rim of Peary (that contains the 4 constantly illuminated areas in our quantitative map) is illuminated. Additionally, so is a portion of the rim of Hermite crater, even though this should nominally be in darkness. This is the same area that was identified in the qualitative Clementine study as potentially tall enough to receive large amounts of continuous sunlight.

**References:** [1] Heiken G. D. et al. (1991) The Lunar Sourcebook CUP 736pp. [2] Bussey D. B. J. et al. (2004) LPSC XXXV, #1387.

## MÖSSBAUER STUDIES IN IMPACTITES FROM HUAMALIES PROVINCE IN HUANCAVELICA REGION, PERU

A. Bustamante<sup>1</sup>, S. Espinoza<sup>1</sup>, G. Morales<sup>2</sup> and  
R. B. Scorzelli<sup>3</sup>. <sup>1</sup>Facultad de Ciencias Físicas,  
Universidad Nacional Mayor de San Marcos,  
Apartado Postal 14-0149, Lima-14, Perú.  
<sup>2</sup>Museo de Historia Natural, Ave. Arenales 1251,  
Lima-11, Peru. <sup>3</sup>Centro Brasileiro de Pesquisas  
Físicas, Rua Dr. Xavier Sigaud 150, RJ, Brasil.  
[abustamante@unmsm.edu.pe](mailto:abustamante@unmsm.edu.pe)

Here we report on Mossbauer studies of three impactite samples denominated PMe-8, PMe-9, and PMe-11 from the Huanuco Region in Peru. The first geological and meteoritical interesting place, in the region, is the locality of Rondobamba, 20 Kms away from Llata's capital, and 300m at the right side of the road, where there is a depression with a crater of 15m diameter and 5-7m deep. The gathered rocky has got extended-pear shape about 15 cms length, with smoothly face and exquisite dark brown color. After a cut, the rock shows a siliconess composition with quartz grains included in a matrix of dark brown color (ferruginous). The surrounding rock of the depression of Yagapasa (sample PMe-9) is a limestone of beige color with layers of horizontal position. The <sup>57</sup>Fe Mössbauer spectra (MS) at RT were obtained in transmission geometry, using a drive operating in triangular mode. Isomer shifts were measured relative to an iron foil. The analysis of the MS spectra reveals an hyperfine magnetic structure with broadened lines, for samples PMe-8 and PMe-9. The spectra were fitted using a distribution model with two (PMe-8) and one (PMe-9) doublets corresponding to aluminum silicates phases. The magnetic hyperfine field obtained was 39T that corresponds to the presence of small particles of goethite. The MS for the sample PME-11 showed a well crystallized hematite ( $B_{hf} \approx 51\text{ T}$ ,  $\varepsilon_Q \approx -0.213$  mm/s, IS=0.378 mm/s). More detailed experiments are in progress.